European Journal of Control xxx (xxxx) xxx

Contents lists available at ScienceDirect

European Journal of Control

journal homepage: www.elsevier.com/locate/ejcon

Online parameters estimation schemes to enhance control performance in DC microgrids

Juan E. Machado[a,1,*], Gianmario Rinaldi[b,1], Michele Cucuzzella[a,c], Prathyush P. Menon[b], Jacquelien M.A. Scherpen[a], Antonella Ferrara[c]

[a] Jan C. Willems Center for Systems and Control, ENTEG, Faculty of Science and Engineering, University of Groningen, Nijenborgh 4, Groningen, 9747 AG, the Netherlands
[b] Department of Engineering, Faculty of Environment, Science and Economy, University of Exeter, N Park Rd, Exeter, EX4 4PY, United Kingdom
[c] Department of Electrical, Computer and Biomedical Engineering, University of Pavia, Via Ferrata 5, Pavia, 27100, Italy

ARTICLE INFO

Article history:
Received 15 May 2023
Accepted 8 June 2023
Available online xxx

Recommended by Prof. T Parisini

Keywords:
DC microgrids
Sliding mode control
Observers for nonlinear systems
Parameters estimation

ABSTRACT

This paper addresses the problem of achieving current sharing and voltage balancing in DC microgrids when the filter parasitic resistances of the Distributed Generation Units (DGUs) are unknown and potentially time-varying. Two schemes are proposed for current sharing and voltage balancing, which use only generated current and voltage measurements. The first scheme is a novel distributed adaptive control utilising the principles of back-stepping and passivity-based control design, intended for the case of constant parasitic resistances. The second scheme alters an existing stabilising controller for current sharing and voltage balancing by incorporating the estimation of the unknown, possibly time-varying, parasitic resistance. A Super-Twisting Sliding Mode Algorithm (STA) estimates the parasitic resistance and its bounded variations in finite-time. The simulation results using a DC microgrid composed of 4 DGUs demonstrate the performance of the proposed schemes.

1. Introduction

Nowadays, it is commonly accepted that microgrids represent a conceptual and technological solution to increase the share of renewable energy sources. A microgrid is in general a low-voltage distribution grid that interconnects Distributed Generation Units (DGUs) and loads [6]. Since several devices such as plug-in electric vehicles, photovoltaic panels and many other electronic applications can be directly connected to DC buses through DC-DC power converters, then DC microgrids have attracted in the last decade, and are still attracting, a great research interest and attention due to their increased efficiency and reliability with respect to the AC counterpart [1].

In order to guarantee a proper and safe operation of the electric devices connected to a DC microgrid, it is crucial to ensure that the grid voltage level is sufficiently close to the nominal one. Moreover, to avoid the over-exploitation of one or more DGUs, it is usually desirable that the overall load demand is shared among all the DGUs proportionally to their generation capacity. This goal is known as proportional *current sharing* [3,20,21]. It is then clear that achieving current sharing is in contrast with ensuring that the voltage at each node of the grid is identically equal to its nominal value. Instead, it has been proposed in the literature to regulate the average voltage across the whole grid towards its nominal value. This second goal is known as *voltage balancing* [3,15,20,21].

A number of solutions have been proposed in the literature to solve the current sharing and the voltage balancing problem; see e.g. the review paper [11] and the references therein. Specifically, in Trip et al. [20], proportional current sharing and voltage balancing are achieved under the assumption that parasitic resistances are negligible or perfectly known, such that their effect can be made negligible by a simple feedforward compensation action. Also, the same control goals have been addressed in Nahata and Ferrari-Trecate [14] via passivity-based control design for the case of constant parasitic resistances with known lower-bounds.

To relax these assumptions, in this paper we propose two novel schemes to estimate the value of the parasitic resistances for DGUs in DC microgrids with Buck converters. The first scheme refers to

* Corresponding author.
E-mail addresses: j.e.machado.martinez@rug.nl (J.E. Machado), g.rinaldi3@exeter.ac.uk (G. Rinaldi), michele.cucuzzella@unipv.it (M. Cucuzzella), p.m.prathyush@exeter.ac.uk (P.P. Menon), j.m.a.scherpen@rug.nl (J.M.A. Scherpen), antonella.ferrara@unipv.it (A. Ferrara).
[1] Juan E. Machado and Gianmario Rinaldi have equally contributed as authors of the present manuscript.

https://doi.org/10.1016/j.ejcon.2023.100860

an adaptive controller that is distributed, and is based on backstepping, adaptive and passivity-based control design tools. Moreover, it offers closed-loop asymptotic stability guarantees under physically sensible assumptions. The second scheme is inspired by a recently published methodology developed by the authors in Rinaldi et al. [17] and is further theoretically developed in this manuscript. The proposed estimator relies on the Sliding Mode (SM) Super-Twisting Algorithm (STA) scheme. SM control techniques have been successfully utilised to solve estimation and control problems in energy networks and microgrids [4,5,9,18,22], as they are insensitive to bounded input disturbances and they enforce finite time convergence of the error [4]. Our scheme is composed of an STA observer to attain the equivalence between DGU generated currents and their estimates. The scheme aims to suitably regulate the value of estimate of the resistance such that the actual value can be estimated *in finite time*. Moreover, we prove that the STA-inspired scheme is capable to track *time-varying* perturbations to the resistance with appropriate modifications in the algorithm. The resistances' estimations are then utilised to modify the controller reported in Kawano et al. [7], Trip et al. [20] with a suitable feed-forward term, making it apt for current sharing and voltage balancing in the scenario where parasitic resistances are non-neglible and time-varying. Compared to the existing solutions available in the literature, our methodology is able to both estimate the unknown resistances in finite time, and accurately track possible changes to the resistance value. Numerical simulations are provided in the paper to assess the performance of the proposed schemes.

The rest of the present paper is structured as follows: Section 2 describes the model and the problem formulation; Section 3 presents the main theoretical key-findings, which are validated via simulations in Sections 4 and 5 concludes the paper.

Notation The notation adopted in this paper is standard. For a given scalar signal x, the expression $\text{sign}(x)$ denotes the sign function. Given two vectors or matrices x, y of the same dimension, the expression $z = x \circ y$ denotes the Hadamard-element-wise product, i.e. each entry of z is defined as $z_{ij} := x_{ij}y_{ij}$. Also, for any $x \in \mathbb{R}^n$ and $P \in \mathbb{R}^{n\times n}$, $\|x\|_P^2 = x^\top Px$. The symbol $\mathbb{I}_n$ denotes the identity matrix of size $n \times n$, whilst 1_n denotes a column vector of size n with all entries equal to 1. The symbol $\text{diag}(x_i)$ denotes a diagonal matrix with its entries x_i.

2. Model and problem formulation

In this section, we describe the setup of the considered DC microgrid and introduce its model. In addition, we formulate the problem that is addressed in this paper and briefly describe the approach we use to solve it.

2.1. Model

We consider a DC microgrid composed of n DGUs and m resistive-inductive power lines. Following [20], the DC microgrid is represented by a connected, simple graph $\mathcal{G} = (\mathcal{N}, \mathcal{E})$, where the nodes $\mathcal{N} = \{1, 2, \dots, n\}$ represent the DGUs, and the edges $\mathcal{E} = \{1, 2, \dots, m\}$, the power lines. As shown in Fig. 1, each DGU voltage source u_i is the main source of energy. Part of this energy is supplied through a Buck converter, with RLC filter, to a local load, absorbing the current $I_{\ell,i}(V_{g,i})$. For any $i \in \mathcal{N}$, the dynamic behaviour of the current through the inductor $L_{g,i}$ and the voltage across the capacitor $C_{g,i}$ is described by the following equations:

$$L_{g,i}\dot{I}_{g,i} = -R_{g,i}I_{g,i} - V_{g,i} + u_i, \tag{1a}$$

$$C_{g,i}\dot{V}_{g,i} = I_{g,i} - I_{\ell,i}(V_{g,i}) - \sum_{k\in\mathcal{E}_i} I_k, \tag{1b}$$

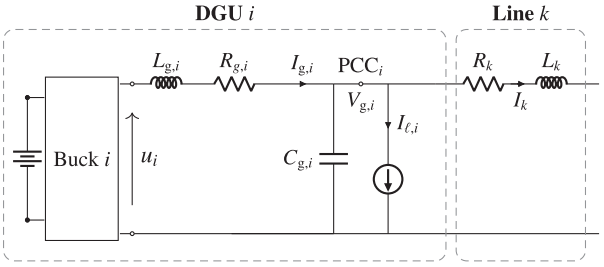

Fig. 1. Electrical scheme of DGU i and line k [20].

where $\mathcal{E}_i \subset \mathcal{E}$ denotes the set of power lines that are incident to $i \in \mathcal{N}$ and through which the ith DGU can exchange power with the neighbouring DGUs. We denote by $I_{g,i}$, $V_{g,i}$ and $R_{g,i}$ the DGU's generated current, the output voltage and the filter resistance, respectively. Also, the current through each power line $k \in \mathcal{E}$ is denoted by I_k, and L_k and R_k are the inductance and resistance of the power line, respectively. Then, the dynamic behaviour of I_k is described by:

$$L_k\dot{I}_k = (V_{g,i} - V_{g,j}) - R_kI_k, \tag{2}$$

where $i, j \in \mathcal{N}$ are the end nodes of k.

Let us assign an arbitrary orientation to the edges of the DC microgrid's graph $\mathcal{G}$ and let $\mathcal{B} \in \mathbb{R}^{n\times m}$ represent the node-edge incidence matrix of $\mathcal{G}$. Then, (1) and (2), can be written in vector form as follows:

$$L_g\dot{I}_g = -R_gI_g - V_g + u, \tag{3a}$$

$$C_g\dot{V}_g = I_g + \mathcal{B}I - I_\ell(V_g), \tag{3b}$$

$$L\dot{I} = -\mathcal{B}^TV_g - RI, \tag{3c}$$

where $I_g = \text{col}(I_{g,i})_{i\in\mathcal{N}}$, $V_g = \text{col}(V_{g,i})_{i\in\mathcal{N}}$ $I = \text{col}(I_k)_{k\in\mathcal{E}}$ and $I_\ell(V_g) := \text{col}(I_{\ell,i}(V_{g,i}))_{i\in\mathcal{N}}$. Moreover, $L_g = \text{diag}(L_{g,i})_{i\in\mathcal{N}}$, $C_g = \text{diag}(L_{g,i})_{i\in\mathcal{N}}$, $R_g = \text{diag}(R_{g,i})_{i\in\mathcal{N}}$, $L = \text{diag}(L_k)_{k\in\mathcal{E}}$ and $R = \text{diag}(R_k)_{k\in\mathcal{E}}$. Concerning the model (3), consider the following:

Assumption 1.

(i) For each DGU, the generated current $I_{g,i}$ and voltage $V_{g,i}$ are locally measured and available for control design purposes. Thus, we define the following control outputs for the system (3):

$$y_1 = I_g, \tag{4a}$$

$$y_2 = V_g. \tag{4b}$$

(ii) There exists a connected and weighted communication graph $\mathcal{G}^{\text{com}} = (\mathcal{N}, \mathcal{E}^{\text{com}}, \mathcal{W}^{\text{com}})$. The Laplacian matrix associated with $\mathcal{G}^{\text{com}}$ is denoted by $\mathcal{L}^{\text{com}}$.

(iii) The electrical loads are combination of constant resistance and constant current loads, i.e.,

$$I_\ell(V_g) = \text{diag}^{-1}(k_z)V_g + k_l, \tag{5}$$

where for each $i \in \mathcal{N}$, $k_{z,i}, k_{l,i} \geq 0$ define the constant resistance and constant current terms of the load, respectively. Moreover, k_z and k_l are *unknown*.

(iv) For each $i \in \mathcal{N}$, the value of the resistance $R_{g,i}$ is unknown but bounded and smoothly time-varying. Moreover, the upper-bound of the first and second time derivatives of $R_{g,i}$ are known.

Remark 1. The unknown parameter $R_{g,i}$ physically represents the LC filter resistance. $R_{g,i}$ is smoothly time-varying in practice, where the variations can be caused by external factors, such as changes in

the ambient temperature, or heating transients due to the thermal losses in the buck converter.

2.2. Problem formulation

The main problem addressed in this paper refers to finding *distributed* controllers for the input u such that the following objectives are satisfied:

Objective 1 (current sharing)**.**

$$\lim_{t\to\infty} I_g = \bar{I}_g, \quad \text{where} \tag{6a}$$

$$w_i \bar{I}_{g,i} = w_j \bar{I}_{g,j}, \ \forall i, j \in \mathcal{N}, \tag{6b}$$

where $w_i > 0$ are weights specified by each DGU.

Objective 2 (voltage balancing)**.**

$$\lim_{t\to\infty} \mathbf{1}_n^\top W^{-1} V_g = \mathbf{1}_n^\top W^{-1} V_g^\star, \tag{7}$$

where $W = \text{diag}(w_i)_{i\in\mathcal{N}}$ and $V_g^\star$ represents, for example, a vector of nominal voltage values for the DGUs.

Let us note that since the DC microgrid graph $\mathcal{G}$ is connected, it follows that $\mathbf{1}_n^\top \mathcal{B} = 0$. Then, the equilibrium condition $C_g \dot{V}_g = 0$ (see (3)) implies that $\mathbf{1}_n^\top \bar{I}_g = \mathbf{1}_n^\top I_\ell(\bar{V}_g)$, i.e., the total current generated by the DGUs must match the total current demand from the loads at the steady-state. However, there are degrees of freedom in the actual current each DGU can inject, which is the main motivation behind Objective 1. The satisfaction of this objective guarantees the regulation of the DGUs currents towards a proportional *current sharing* regime defined by the weighting factors w_i. Note that if the value of w_i, $i \in \mathcal{N}$, is chosen to be inversely proportional to its respective DGU capacity, then the DGUs with higher capacities will have higher current values in steady-state. Concerning Objective 2, note from the equilibrium condition $L\dot{I} = 0$ (see (3)) that the vectors V_g and I satisfy, at steady-state, the equation

$$0 = -\mathcal{B}^\top \bar{V}_g - R\bar{I}.$$

Due to the properties of $\mathcal{B}$, $\bar{V}_g$ can in fact be shifted by the vector $a\mathbf{1}_n$ for any $a \in \mathbb{R}$. That is, it is possible to find $\bar{u}$ such that $\bar{V}_g + a\mathbf{1}_n$ is also an equilibrium voltage. This is the motivation behind Objective 2, which will guarantee the regulation of all DGUs *average voltage* towards the average of the voltage constant reference $V_g^\star$.

Remark 2. The denomination "distributed" for the desired control design means that the control law for each u_i should depend only on measurements and data that are locally available, e.g., $I_{g,i}$ and $L_{g,i}$. Moreover, in view of Assumption 1, the exchange of measurement data between two adjacent nodes of the communication graph $\mathcal{G}^{\text{com}}$ is also allowed.

3. Main results

In this section, we present two schemes for achieving Objectives 1 and 2 whilst estimating the resistance R_g online. First, we treat the case of constant R_g, for which an adaptive scheme is proposed. Then, we move on to the case of time-varying R_g, for which we design an observer based on sliding modes.

3.1. Case of constant R_g

In the following proposition we propose a distributed, adaptive controller that achieves Objectives 1 and 2 for the case when R_g is constant, yet *unknown*.

Proposition 1. *Consider the microgrid model (3) under Assumption 1. (i)–(iii) and further assume that $k_{z,i} > 0$ for each $i \in \mathcal{N}$ and that $R_{g,i} > 0$ is constant. Let us introduce the variable z_g as follows*

$$z_g := I_g - \varphi_g \tag{8}$$

and design the control input u as

$$T_{\varphi_g}\dot{\varphi}_g = -(V_g - V_g^\star) - W\mathcal{L}^{\text{com}}\theta_g, \tag{9a}$$

$$T_{\theta_g}\dot{\theta}_g = \mathcal{L}^{\text{com}} W (z_g + \varphi_g), \tag{9b}$$

$$T_{\hat{r}_g}\dot{\hat{r}}_g = -\text{diag}(z_g + \varphi_g) z_g, \tag{9c}$$

$$\begin{aligned} u = &-K_{z_g} z_g + \text{diag}(\hat{r}_g)(z_g + \varphi_g) + V_g^\star \\ &+ L_g T_{\varphi_g}^{-1}\big(-(V_g - V_g^\star) - W\mathcal{L}^{\text{com}}\theta_g\big) \\ &- W\mathcal{L}^{\text{com}}\theta_g, \end{aligned} \tag{9d}$$

where $K_{z_g}, T_{\varphi_g}, T_{\theta_g}, T_{\hat{r}_g} \in \mathbb{R}^{n\times n}$ are positive-definite diagonal matrices of control parameters. Then, the closed-loop system, formed by (3) and (9), can be equivalently written as

$$\begin{aligned} L_g\dot{z}_g = &-K_{z_g} z_g + \text{diag}(\varphi_g + z_g)(\hat{r}_g - R_g\mathbf{1}_n) \\ &- (V_g - V_g^\star) - W\mathcal{L}^{\text{com}}\theta_g, \end{aligned} \tag{10a}$$

$$C_g\dot{V}_g = z_g + \varphi_g + \mathcal{B}I - \text{diag}^{-1}(k_z)V_g - k_l, \tag{10b}$$

$$L\dot{I} = -\mathcal{B}^\top V_g - RI, \tag{10c}$$

$$T_{\varphi_g}\dot{\varphi}_g = -(V_g - V_g^\star) - W\mathcal{L}^{\text{com}}\theta_g, \tag{10d}$$

$$T_{\theta_g}\dot{\theta}_g = \mathcal{L}^{\text{com}} W (z_g + \varphi_g), \tag{10e}$$

$$T_{\hat{r}_g}\dot{\hat{r}}_g = -\text{diag}(\varphi_g + z_g) z_g. \tag{10f}$$

Moreover, if (10) admits an equilibrium point, say $(\bar{z}_g, \bar{V}_g, \bar{I}, \bar{\varphi}_g, \bar{\theta}_g, \bar{\hat{r}}_g)$, then such equilibrium point is globally asymptotically stable, Objectives 1 and 2 are achieved, and $\bar{\hat{r}}_g = R_g\mathbf{1}_n$.

Proof. Let us begin by introducing the change of variable from I_g to z_g as shown in (8). Then, we can compute $L_g\dot{z}_g$ as follows:

$$\begin{aligned} L_g\dot{z}_g &= L_g\dot{I}_g - L_g\dot{\varphi}_g \\ &= (-R_g I_g - V_g + u) - L_g T_{\varphi_g}^{-1}\big(-(V_g - V_g^\star) - W\mathcal{L}^{\text{com}}\theta_g\big), \end{aligned} \tag{11}$$

where we have substituted $L_g\dot{I}_g$ from (3) and $\dot{\varphi}_g$ from (9). Now we substitute into (11) the value of u shown in (9), to obtain:

$$\begin{aligned} L_g\dot{z}_g &= -R_g I_g - V_g - K_{z_g}(I_g - \varphi_g) + \text{diag}(\hat{r}_g) I_g + V_g^\star \\ &\quad - W\mathcal{L}^{\text{com}}\theta_g \\ &= \text{diag}(I_g)(\hat{r}_g - r_g) - (V_g - V_g^\star) - K_{z_g}(I_g - \varphi_g) \\ &\quad - W\mathcal{L}^{\text{com}}\theta_g, \end{aligned} \tag{12}$$

where we have used $r_g := R_g\mathbf{1}_n$ and the identity $\big(\text{diag}(\hat{r}_g) - R_g\big)I_g = \text{diag}(I_g)\big(\hat{r}_g - R_g\mathbf{1}_n\big)$. By propagating the change of variable (8) to (12) and the V_g-dynamics of the microgrid in (3), we get that the closed-loop system is equivalent to (10), where we have substituted the value of I_ℓ from (5). By direct substitution, it can be verified that if (10) admits an equilibrium point, which we denote by $(\bar{z}_g, \bar{V}_g, \bar{I}, \bar{\varphi}_g, \bar{\theta}_g, \bar{\hat{r}}_g)$, then the equilibrium conditions $L_g\dot{z}_g = 0$, $T_{\varphi_g}\dot{\varphi}_g = 0$ and $T_{\hat{r}_g}\dot{\hat{r}}_g = 0$, together with the *fact* that $\bar{\varphi}_{g,i} + \bar{z}_{g,i} > 0$ for all $i \in \mathcal{N}$ (see Remark 4), imply that $\bar{z}_g = 0_n$. This in turn implies from the condition $T_{\theta_g}\dot{\bar{\theta}}_g = 0$ that

$$\mathcal{L}^{\text{com}} W \bar{\varphi}_g = \mathcal{L}^{\text{com}} W \bar{I}_g = 0 \tag{13}$$

and

$$\bar{\hat{r}}_g = R_g\mathbf{1}_n. \tag{14}$$

Moreover, the equilibrium condition $T_{\varphi_g}\dot{\bar{\varphi}}_g = 0$ implies that $\mathbf{1}_n^\top W^{-1}\left(-(\bar{V}_g - V_g^\star) - W\mathcal{L}^{\text{com}}\bar{\theta}_g\right) = 0$, or equivalently, that

$$\mathbf{1}_n^\top W^{-1}\bar{V}_g = \mathbf{1}_n^\top W^{-1}V_g^\star. \tag{15}$$

In view of (13) and (15), to achieve Objectives 1 and 2, it is sufficient to show that the equilibrium $(\bar{z}_g, \bar{V}_g, \bar{I}, \bar{\varphi}_g, \bar{\theta}_g, \bar{\hat{r}}_g)$ is asymptotically stable. To assess the stability of this equilibrium, consider the following Lyapunov function candidate

$$\begin{aligned} S = &\frac{1}{2}\|z_g\|^2_{L_g} + \frac{1}{2}\|V_g - \bar{V}_g\|^2_{C_g} + \frac{1}{2}\|I - \bar{I}\|^2_L + \frac{1}{2}\|\varphi_g - \bar{\varphi}_g\|^2_{T_{\varphi_g}} \\ &+ \frac{1}{2}\|\theta_g - \bar{\theta}_g\|^2_{T_{\theta_g}} + \frac{1}{2}\|\hat{r}_g - \bar{\hat{r}}_g\|^2_{T_{\hat{r}_g}}, \end{aligned} \tag{16}$$

which is positive-definite with respect to the equilibrium under consideration. Moreover, the time derivative of S, along trajectories of (10), satisfies:

$$\begin{aligned} \dot{S} = &z_g^\top L_g\dot{z}_g + (V_g - \bar{V}_g)^\top C_g\dot{V}_g + (I - \bar{I})^\top L\dot{I} + \\ &+ (\varphi_g - \bar{\varphi}_g)^\top T_{\varphi_g}\dot{\varphi}_g + (\theta_g - \bar{\theta}_g)^\top T_{\theta_g}\dot{\theta}_g \\ &+ (\hat{r}_g - \bar{\hat{r}}_g)^\top T_{\hat{r}_g}\dot{\hat{r}}_g. \end{aligned} \tag{17}$$

Since the equilibrium being analysed makes the right-hand side of (10) zero, then we can write (10) equivalently as follows:

$$L_g\dot{z}_g = -K_{z_g}z_g + \text{diag}(\varphi_g + z_g)(\hat{r}_g - \bar{\hat{r}}_g) \tag{18a}$$

$$- (V_g - \bar{V}_g) - W\mathcal{L}^{\text{com}}(\theta_g - \bar{\theta}_g), \tag{18b}$$

$$C_g\dot{V}_g = z_g + (\varphi_g - \bar{\varphi}_g) + \mathcal{B}(I - \bar{I}) - \text{diag}(k_z)(V_g - \bar{V}_g), \tag{18c}$$

$$L\dot{I} = -\mathcal{B}^\top(V_g - \bar{V}_g) - R(I - \bar{I}), \tag{18d}$$

$$T_{\varphi_g}\dot{\varphi}_g = -(V_g - \bar{V}_g) - W\mathcal{L}^{\text{com}}(\theta_g - \bar{\theta}_g), \tag{18e}$$

$$T_{\theta_g}\dot{\theta}_g = \mathcal{L}^{\text{com}}Wz_g + \mathcal{L}^{\text{com}}W(\varphi_g - \bar{\varphi}_g), \tag{18f}$$

$$T_{\hat{r}_g}\dot{\hat{r}}_g = -\text{diag}(\varphi_g + z_g)z_g. \tag{18g}$$

Consequently, $\dot{S}$ in (17) can further be simplified into the expression:

$$\dot{S} = -\|z_g\|^2_{K_{z_g}} - \|V_g - \bar{V}_g\|^2_{\text{diag}^{-1}(k_z)} - \|I - \bar{I}\|^2_R. \tag{19}$$

Since $\dot{S} \leq 0$, the stability of the equilibrium $(\bar{z}_g, \bar{V}_g, \bar{I}, \bar{\varphi}_g, \bar{\theta}_g, \bar{\hat{r}}_g)$ is concluded. To show asymptotic stability, we invoke LaSalle's invariance theorem. Then, it is sufficient to show that the $(\bar{z}_g, \bar{V}_g, \bar{I}, \bar{\varphi}_g, \bar{\theta}_g, \bar{\hat{r}}_g)$ is the largest invariant set of (18) in which $\dot{S}$ is zero all the time. This is done next.

Let $(z_g, V_g, I, \varphi_g, \theta_g, \hat{r}_g)$ be any solution of (10) which satisfies $\dot{S} = 0$ all the time. Then, $z_g = \bar{z}_g = 0$, $V_g = \bar{V}_g$ and $I = \bar{I}$ all the time. Under these conditions, the equilibrium condition $C_g\dot{V}_g = 0$ (see (18)) leads to establish that $\varphi_g = \bar{\varphi}_g$ all the time. Since $z_g = 0$ and $\varphi_g = \bar{\varphi}_g$, it follows from (18) that $T_{\theta_g}\dot{\theta}_g = 0$, i.e., θ_g is constant. In fact, $\theta_g = \bar{\theta}_g$, which can be directly established from the equilibrium condition $T_{\varphi_g}\dot{\varphi}_g = 0 \Rightarrow 0 = \mathcal{L}^{\text{com}}(\theta_g - \bar{\theta}_g)$ and from the fact that $1^\top T_{\theta_g}\dot{\theta}_g = 0 \Rightarrow 1^\top T_{\theta_g}\theta_g = 1^\top T_{\theta_g}\theta_g(0)\ \forall t \geq 0$; see (18). Finally, from the equilibrium condition $L_g\dot{z}_g = 0$ we get that $\hat{r} = \bar{\hat{r}}_g$ all the time, where we have used the assumption $\bar{\varphi}_{g,i} + \bar{z}_{g,i} = \bar{I}_{g,i} > 0$. Therefore, the equilibrium $(\bar{z}_g, \bar{V}_g, \bar{I}, \bar{\varphi}_g, \bar{\theta}_g, \bar{\hat{r}}_g)$ is the largest invariant set of (10) in which the time derivative of the positive-definite, and non-increasing function S is identically zero. Hence, the equilibrium in question is asymptotically stable by virtue of LaSalle's invariance principle (see, e.g., Khalil [8, Th. 3.5]. Consequently, Objectives 1 and 2 are fulfilled. Also, from (14), we have that $\lim_{t\to\infty}\hat{r}_g = R_g\mathbf{1}_n$. □

Remark 3. The controller u in (9) is obtained in two steps. The first one consists in defining the backstepping-inspired change of variable in (8) (see, e.g., Khalil [8, Ch. 9]), which allows to introduce an integral action in the "non-actuated" state V_g, the dynamics of which are subject to the constant disturbance k_I. The second step consists in choosing u such that the overall closed-loop system, with dynamic extensions φ_g, θ_g and $\hat{r}_g$, has a port-Hamiltonian representation, which are features of the IDA-PBC control design methodology (see Astolfi and Ortega [2], Ortega and Garcia-Canseco [16]). Here we omit the port-Hamiltonian representation, but the interested reader is referred to the proof of Proposition 2 in Machado et al. [10] for a similar design and analysis. Nonetheless, we specify that the dynamic extension φ_g allows to meet Objective 2. Moreover, the introduction of the θ_g-dynamics permits to achieve Objective 1, as it is evident from the equilibrium condition associated with these dynamics. Finally, the $\hat{r}_g$-dynamics is the adaptive feature of our design, as it leads to the estimation of the unknown resistance matrix R_g (c.f. Nageshrao et al. [13, Ex. 4]).

Remark 4. The fact that the equilibrium value $\bar{\varphi}_{g,i} + \bar{z}_{g,i} = \bar{I}_{g,i}$ is positive for all $i \in \mathcal{N}$ invoked in the proof of Proposition 1 guarantees, in particular, that $\lim_{t\to\infty}\hat{r}_g = R_g\mathbf{1}_n$, i.e., the unknown resistance matrix R_g can be accurately estimated, the exact compensation of which is central to the carried out asymptotic stability analysis. We note that the equilibrium condition $\bar{\varphi}_{g,i} + \bar{z}_{g,i} = \bar{I}_{g,i} > 0$, for all $i \in \mathcal{N}$, is ensured from two facts: (i) the total current generated by the DGUs must match the total current demand from the loads at the steady-state ($\Rightarrow I_{g,k} > 0$, for some $k \in \mathcal{N}$); and (ii) the equalities $0 = \mathcal{L}^{\text{com}}W(\bar{z}_g + \bar{\varphi}_g) = \mathcal{L}^{\text{com}}W\bar{I}_g$, which imply (6), hold at steady-state.

3.2. Extension to the case of time-varying R_g

In this subsection, we introduce an observer based on the STA for the finite time online estimation of R_g, which henceforth is assumed to be time-varying (see Assumption 1.(iv)). Subsequently, we explain how such an estimate for R_g can be coupled with a slightly modified version of the passivity-based controller reported in Trip et al. [20] where Objectives 1 and 2 are achieved only in the scenario where $R_g = 0$.

In order to introduce the assumptions needed in the design of the observer for R_g, first we present the controller proposed in Trip et al. [20], i.e.,

$$T_\theta\dot{\theta} = -\mathcal{L}^{\text{com}}WI_g, \tag{20a}$$

$$T_\phi\dot{\phi} = -\phi + I_g, \tag{20b}$$

$$u = -K(I_g - \phi) + W\mathcal{L}^{\text{com}}\theta + V_g^\star, \tag{20c}$$

where $T_\theta, T_\phi, K \in \mathbb{R}^{n\times n}$ are positive-definite diagonal matrices of control parameters and W is a diagonal matrix as defined in Objective 2.

Some properties of the controller (20) are as follows [20]:

- The right-hand side of the θ-dynamics is an algorithm for the weighted consensus of the DGUs currents. It is often used in power systems control design to achieve *fair* current sharing among DGUs, as the equilibrium current vector $\bar{I}_g$ necessarily satisfies $W\bar{I}_g \propto \mathbf{1}_n$, which is equivalent to (6b).
- The introduction of the variable ϕ, which acts as a filter on I_g, but without altering its desired equilibrium value, is useful to attenuate oscillations. In addition, the state-feedback term $-K(I_g - \phi)$ in u is fundamental to guarantee convergence of solutions of the closed-loop system towards a *constant* steady-state.

- Finally, the term $W\mathcal{L}^{\text{com}}\theta + V_{\text{g}}^{\star}$ comes from the desire of establishing a *passive* (or skew-symmetric) interconnection between the I_{g}-dynamics and the θ-dynamics, while simultaneously achieving Objective 2. Indeed, note that if $R_{\text{g}} = 0$ all the time, the I_{g}-dynamics of (3) in closed-loop with (20) becomes:

$$L_{\text{g}}\dot{I}_{\text{g}} = -K(I_{\text{g}} - \phi) + W\mathcal{L}^{\text{com}}\theta - (V_{\text{g}} - V_{\text{g}}^{\star}). \tag{21}$$

  Therefore, at the steady-state the identity $W\mathcal{L}^{\text{com}}\bar{\theta} - (\bar{V} - V_{\text{g}}^{\star}) = 0$ holds (as $\bar{I}_{\text{g}} = \bar{\phi}_{\text{g}}$). After (pre) multiplication by $\mathbf{1}_n^{\top}W^{-1}$, it leads to (7).

Even though the controller (20) fulfils Objectives 1 and 2 in the scenario when R_{g} is equal to zero, this is not the case when $R_{\text{g}} > 0$, even if its value is constant. To see this, assume that $R_{\text{g}} > 0$ and constant. Then, the I_{g}-dynamics of (3) in closed-loop with (20) is given by:

$$L_{\text{g}}\dot{I}_{\text{g}} = -R_{\text{g}}I_{\text{g}} - K(I_{\text{g}} - \phi) + W\mathcal{L}^{\text{com}}\theta - (V_{\text{g}} - V_{\text{g}}^{\star}).$$

Then, at steady-state we obtain $-R_{\text{g}}\bar{I}_{\text{g}} + W\mathcal{L}^{\text{com}}\theta - (V_{\text{g}} - V_{\text{g}}^{\star}) = 0$, which, after (pre) multiplication by $\mathbf{1}_n^{\top}W^{-1}$, leads to $\mathbf{1}_n^{\top}W^{-1}\bar{V}_{\text{g}} = \mathbf{1}_n^{\top}W^{-1}\bar{V}_{\text{g}}^{\star} - \mathbf{1}_n^{\top}W^{-1}R_{\text{g}}\bar{I}_{\text{g}}$. Then, (7) holds only if $\bar{I}_{\text{g}} = 0$, which is not desired. To overcome this limitation, and considering also the case where R_{g} is time-varying, next we design an observer scheme to estimate in finite time the value of R_{g}, which will be then used in (20) to cancel the term $-R_{\text{g}}I_{\text{g}}$ in the I_{g}-dynamics (3).

3.2.1. Finite time estimation of $R_{\text{g}}(t)$

We introduce an STA to estimate in finite time the time-varying resistance R_{g}. To this end, consider the assumption:

Assumption 2. All solutions of the microgrid model (3), subject to Assumption 1, in closed-loop with (20), are bounded all the time.

The estimation scheme is then defined in the following proposition:

Proposition 2. *Consider the microgrid model (3a) under Assumptions 1 and 2, and the following* ***STA observer***

$$L_{\text{g}}\dot{\hat{I}}_{\text{g}} = -\hat{R}_{\text{g}}y_1 + y_2 + u + L_{\text{g}}f_1(\tilde{I}_{\text{g}}) + L_{\text{g}}\hat{\nu}, \tag{22a}$$

$$\dot{\hat{\nu}} = f_2(\tilde{I}_{\text{g}}), \tag{22b}$$

$$\hat{y}_1 = \hat{I}_{\text{g}}, \tag{22c}$$

where $\hat{R}_{\text{g}} := \text{diag}(\hat{R}_{\text{g},i})_{i\in\mathcal{N}}$, with the scalar entry $\hat{R}_{\text{g},i}$ representing an estimate of the ith resistance. We define the output observation error as $\tilde{I}_{\text{g}} := \hat{y}_1 - y_1$. Each component of $\tilde{I}_{\text{g}}$ is given by $\tilde{I}_{\text{g},i} := \hat{I}_{\text{g},i} - I_{\text{g},i}$, $i \in \mathcal{N}$. The two nonlinear functions $f_1(\cdot)$, $f_2(\cdot)$ are defined by the STA structure as:

$$f_1(\tilde{I}_{\text{g}}) := \text{col}\left(-\alpha_{1,i}|\tilde{I}_{\text{g},i}|^{\frac{1}{2}}\text{sign}(\tilde{I}_{\text{g},i})\right)_{i\in\mathcal{N}} \tag{22d}$$

$$f_2(\tilde{I}_{\text{g}}) := \text{col}\left(-\alpha_{2,i}\text{sign}(\tilde{I}_{\text{g},i})\right)_{i\in\mathcal{N}} \tag{22e}$$

and $\alpha_{1,i}$ and $\alpha_{2,i}$ are positive design parameters. To regulate the convergence of $\hat{R}_{\text{g}}$ to R_{g}, an additional ***STA scheme*** *is proposed as follows:*

$$\sigma_{R_{\text{g}}} = -L_{\text{g}}\hat{\nu} \circ \check{y}_1 \tag{22f}$$

$$\hat{R}_{\text{g}} = \int_0^t \varphi d\tau \qquad \hat{R}_{\text{g}}(0) = R_{0_{\text{g}}} \tag{22g}$$

$$\varphi := \text{diag}(\varphi_i)_{i\in\mathcal{N}} \tag{22h}$$

$$\varphi_i = \begin{cases} 0 & \text{if} \quad |\tilde{I}_{\text{g},i}| > 0 \\ \xi_i & \text{else} \end{cases} \tag{22i}$$

where $\sigma_{R_{\text{g}}}$ is the sliding variable of the STA scheme, $\check{y}_1 := \text{col}(1/y_{1i})_{i\in\mathcal{N}}$, $\hat{R}_{\text{g}}(0) = R_{0_{\text{g}}}$ is the initial condition of $\hat{R}_{\text{g}}$. Once the sliding mode of the STA scheme (22a)–(22c) is enforced, it follows that $|\tilde{I}_{\text{g},i}| = 0$, and the identity $\varphi_i = \dot{\hat{R}}_{\text{g},i} \equiv \xi_i$ holds. The evolution of ξ is therefore governed as follows:

$$\xi = g_1(\sigma_{R_{\text{g}}}) + \omega \tag{22j}$$

$$\dot{\omega} = g_2(\sigma_{R_{\text{g}}}), \quad \omega(0) = \omega_0, \tag{22k}$$

where $\omega := \text{col}(\omega_i)_{i\in\mathcal{N}}$ is an auxiliary variable, and the nonlinear functions $g_1(\cdot)$ and $g_2(\cdot)$ are

$$g_1(\sigma_{R_{\text{g}}}) := \text{col}\left(-\beta_{1,i}|\sigma_{R_{\text{g},i}}|^{\frac{1}{2}}\text{sign}(\sigma_{R_{\text{g},i}})\right)_{i\in\mathcal{N}} \tag{22l}$$

$$g_2(\sigma_{R_{\text{g}}}) := \text{col}\left(-\beta_{2,i}\text{sign}(\sigma_{R_{\text{g},i}})\right)_{i\in\mathcal{N}} \tag{22m}$$

and $\beta_{1,i}$ and $\beta_{2,i}$ are positive design constants. Then, the condition

$$\hat{R}_{\text{g}} = R_{\text{g}} \tag{23}$$

is enforced in ***a finite time****.*

Proof. The STA observer (22a)–(22c) is designed to ensure the convergence to the origin of $\tilde{I}_{\text{g}}$. By subtracting (3a) from (22a), and multiplying the result by the diagonal matrix L_{g}^{-1} it yields an explicit expression of the error dynamics as

$$\dot{\tilde{I}}_{\text{g}} = L_{\text{g}}^{-1}\Big(-\hat{R}_{\text{g}} + R_{\text{g}}\Big)y_1 + f_1(\tilde{I}_{\text{g}}) + \hat{\nu} \tag{24a}$$

$$\dot{\hat{\nu}} = f_2(\tilde{I}_{\text{g}}). \tag{24b}$$

We define a function $\rho(\cdot)$ as

$$\rho(\cdot) := L_{\text{g}}^{-1}\Big(-\hat{R}_{\text{g}} + R_{\text{g}}\Big)y_1 = L_{\text{g}}^{-1}\tilde{R}_{\text{g}} \circ y_1, \tag{25}$$

where the auxiliary error variables are $\tilde{R}_{\text{g},i} := \hat{R}_{\text{g},i} - R_{\text{g},i}$, $\tilde{R}_{\text{g}} := \text{col}(\tilde{R}_{\text{g},i})_{i\in\mathcal{N}}$. If we introduce also the error variable

$$\tilde{I}_{2_{\text{g}}} := \rho(\cdot) + \hat{\nu}, \tag{26}$$

we obtain

$$\dot{\tilde{I}}_{\text{g}} = \tilde{I}_{2_{\text{g}}} + f_1(\tilde{I}_{\text{g}}) \tag{27a}$$

$$\dot{\tilde{I}}_{2_{\text{g}}} = f_2(\tilde{I}_{\text{g}}) + \dot{\rho}(\cdot). \tag{27b}$$

The system in (27a) and (27b) is in the conventional STA structure [12]. Under Assumption 1, the function $\rho(\cdot)$ and its derivative are composed of bounded contributions, and therefore

$$|\dot{\rho}_i(\cdot)| < \Delta_{\rho_i} \tag{28}$$

where Δ_{ρ_i} is a known positive constant. If each pair of design parameters satisfy the following tuning rules [12,19]:

$$\alpha_{1,i} = 1.5\sqrt{\Delta_{\rho_i}} \tag{29}$$

$$\alpha_{2,i} = 1.1\Delta_{\rho_i} \tag{30}$$

the error dynamics converge to the origin in finite time. Exploiting the definition of (25), assuming that $y_1 > 0$, we can note that each entry $\rho_i(\cdot)$ of the vector $\rho(\cdot)$ satisfies

$$\rho_i(\cdot)\begin{cases} >0 & \text{if} \quad \tilde{R}_{\text{g},i} > 0 \\ =0 & \text{if} \quad \tilde{R}_{\text{g},i} = 0 \\ <0 & \text{if} \quad \tilde{R}_{\text{g},i} < 0 \end{cases} \tag{31}$$

Therefore, $\rho(\cdot) = 0$ if an only if all the components of the error $\tilde{R}_{\text{g}}$ are equal to zero. During the sliding phase of the error system

(27a) and (27b), a real-time estimate $\hat{\rho}(\cdot)$ for $\rho(\cdot)$ can be extracted as

$$\hat{\rho}(\cdot) = -\hat{v}. \tag{32}$$

Inspired by [17], we select the following variable

$$\sigma_{R_g} := -L_g \hat{v} \circ \check{y}_1 = L_g L_g^{-1} \tilde{R}_g y_1 \circ \check{y}_1 = \tilde{R}_g \tag{33}$$

to be nullified in finite time. Under the STA structure regulating $\hat{R}_g$ in (22f)–(22k), from (31) and under the equality derived in (33), the error system

$$\dot{\sigma}_{R_g} = g_1(\sigma_{R_g}) + \omega - \psi(R_g), \tag{34a}$$

$$\dot{\omega} = g_2(\sigma_{R_g}), \tag{34b}$$

can be derived, where $\psi(R_g) := \mathrm{col}(\dot{R}_{g,i})_{i\in\mathcal{N}}$. If we define the error variable $e_{2_{R_g}} := \omega - \psi(R_g)$, it follows that

$$\dot{\sigma}_{R_g} = g_1(\sigma_{R_g}) + e_{2R_g}, \tag{35a}$$

$$\dot{e}_{2_{R_g}} = g_2(\sigma_{R_g}) + \dot{\psi}(R_g). \tag{35b}$$

The system in (35a) and (35b) exhibits a STA structure. Under Assumption 1, each component of $\dot{\psi}(R_g)$ satisfies:

$$|\dot{\psi}_i(R_{g,i})| \equiv |\ddot{R}_{g,i}| < \Delta_{R_{g,i}}. \tag{36}$$

The system (35a) and (35b) converges to the origin in finite time provided that $\beta_{1,i} = 1.5\sqrt{\Delta_{R_{g,i}}}$ and $\beta_{2,i} = 1.1\Delta_{R_{g,i}}$ [4,12]. The condition $\hat{R}_{g,i} = R_{g,i}$ holds in finite time also. □

Remark 5. Note that the upper-bound of the finite time required for the convergence can be computed as follows: $t_i^{\mathrm{sm}} = c_t \mathcal{V}_i(\sigma_{R_{g,i}}(0))$, where $\mathcal{V}_i$ is the Lyapunov function proposed in Moreno [12].

3.2.2. Achieving Objectives 1 and 2 in the case of time-varying R_g

In this part of the paper, we combine the finite-time estimation scheme for R_g in Proposition 2 with the controller (20) in order to achieve Objectives 1 and 2. First, consider the following assumption:

Assumption 3. The quantity $t^{\mathrm{sm}} := \max_{i\in\mathcal{N}}\{t_i^{\mathrm{sm}}\}$, where t_i^{sm} is determined by each DGU, is available to all the microgrid DGUs.

Therefore, the main result of this subsection is the following:

Proposition 3. *Consider the microgrid model (3) in closed-loop with (20) and subject to Assumptions 1–3. For $t \geq t^{\mathrm{sm}}$, modify the controller (20) by adding the term $+\hat{R}_g I_g$ to u, where $\hat{R}_g$ is the estimate of R_g obtained through Proposition 2. Then, from $t \geq t^{\mathrm{sm}}$, the closed-loop system, with the modified controller, is globally asymptotically stable and satisfies Objectives 1 and 2.*

Proof. In view of Assumption 2, all trajectories of (3) in closed-loop with (20) remain bounded between $0 \leq t < t^{\mathrm{sm}}$. For $t \geq t^{\mathrm{sm}}$, we have from Proposition 2 that $\hat{R}_g = R_g$. Hence the controller (20) with $\hat{R}_g I_g$ added to u will effectively cancel the term $-R_g I_g$ in the closed-loop system's I_g-dynamics (see (21)). From here on, the proof follows from Trip et al. [20, Th. 1]. □

Remark 6. The computation of t^{sm} in Assumption 3 depends on the closed-loop system initial conditions, which in practice might require the exchange of system-wide information among the DGUs. A potentially conservative alternative to that, consists in locally computing, offline, upper bounds for each t_i^{sm} in a set of feasible system initial conditions.

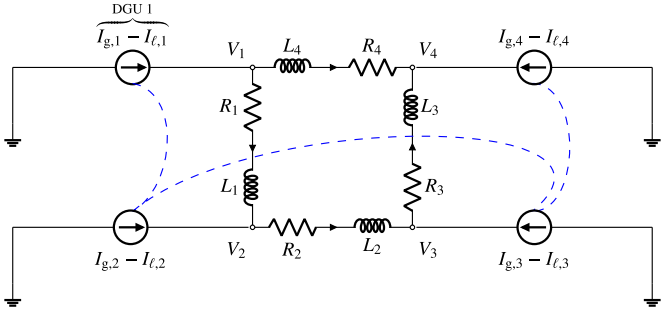

Fig. 2. Scheme of the considered DC microgrid with 4 DGUs. The dashed lines represent the communication network. Figure courtesy of Trip et al. [20].

4. Simulations

In this section, we assess the performance of the proposed estimation and control schemes via numerical simulations. The considered DC microgrid is composed of 4 DGUs, as depicted in Fig. 2. The simulations are executed in a MATLAB-Simulink R2021b environment. The prototypical model parameters have been taken from Cucuzzella et al. [3]. The parameters of the control scheme (9a)–(9d) are chosen as: $T_{\varphi_g} = 0.02\mathbb{I}_4$, $T_{\theta_g} = 0.02\mathbb{I}_4$, $T_{\hat{\Gamma}_g} = 0.02\mathbb{I}_4$, $W = \mathbb{I}_4$, $K_{z_g} = 100\mathbb{I}_4$. The parameters of the STA observer (22a)–(22c) are set equal to $\alpha_{1,i} = 42.60$, $\alpha_{2,i} = 2250$, whilst those of the STA scheme (22f)–(22i) are $\beta_{1,i} = 69.57$, $\beta_{2,i} = 6000$. The initial values for the time-varying matrix R_g are set equal to

$$R_g(0) = \mathrm{diag}(0.2,\ 0.3,\ 0.5,\ 0.1)\ \ (\Omega)$$

The matrix $R_g(t)$ evolves according to the following law:

$$R_g(t) := R_g(0) + \Psi(t) + \Lambda(t) \tag{37}$$

where the perturbations $\Psi(t)$ and $\Lambda(t)$ are: $\Psi(t) = \sin(\pi t)$ diag $[0.02,\ 0.01,\ -0.01,\ -0.02]$, and $\Lambda(t) = (1 - e^{-\frac{t}{4}})$ diag $[0.06,\ 0.03,\ -0.03,\ 0.06]^\top$. The matrix $\Psi(t)$ models low-frequency oscillatory behaviour of R_g, whilst $\Lambda(t)$ captures an exponential transient. In this study, the time evolution of $R_g(t)$ is caused by unmodelled exogenous processes, such as temperature variation. The simulations are executed with a time duration of $T_{\mathrm{sim}} = 10$ s. To quantitatively account for the performance of the proposed schemes, the following Root-Mean Square Error (RMSE) performance metrics are introduced:

$$\mathcal{M}_{R_g} := \frac{1}{T_{\mathrm{sim}} - t^{\mathrm{sm}}} \int_0^{T_{\mathrm{sim}}} ||\tilde{R}_g(\tau)||_2 \, d\tau \tag{38}$$

$$\mathcal{M}_{V_g} := \frac{1}{T_{\mathrm{sim}} - t^{\mathrm{sm}}} \int_0^{T_{\mathrm{sim}}} ||\mathbf{1}_n^\top W^{-1}(V_g(\tau) - V_g^\star)||_2 \, d\tau \tag{39}$$

The metric $\mathcal{M}_{R_g}$ accounts for the global accuracy in the estimation of R_g, whilst the metric $\mathcal{M}_{V_g}$ accounts for the global voltage regulation performance. Four scenarios are considered:

- **Scenario (A)**, where the matrix R_g remains *constant*, and the scheme (9a)–(9d) is employed to achieve current sharing and voltage balancing.
- **Scenario (B)**, where the matrix R_g is time-varying according to (37), and the compensation scheme (9a)–(9d) is still employed.
- **Scenario (C)**, where the matrix R_g is time-varying according to (37), and the control scheme (22a)–(22c), (22f)–(22i) is employed *without* a resistance estimation compensation.
- **Scenario (D)**, where the matrix R_g is time-varying according to (37), and the compensation scheme (22a)–(22c), (22f)–(22i) implemented as per Proposition 3 is employed.

For each introduced scenario, we consider also the impact of Gaussian white measurement noises on the state variables I_g, V_g, I.

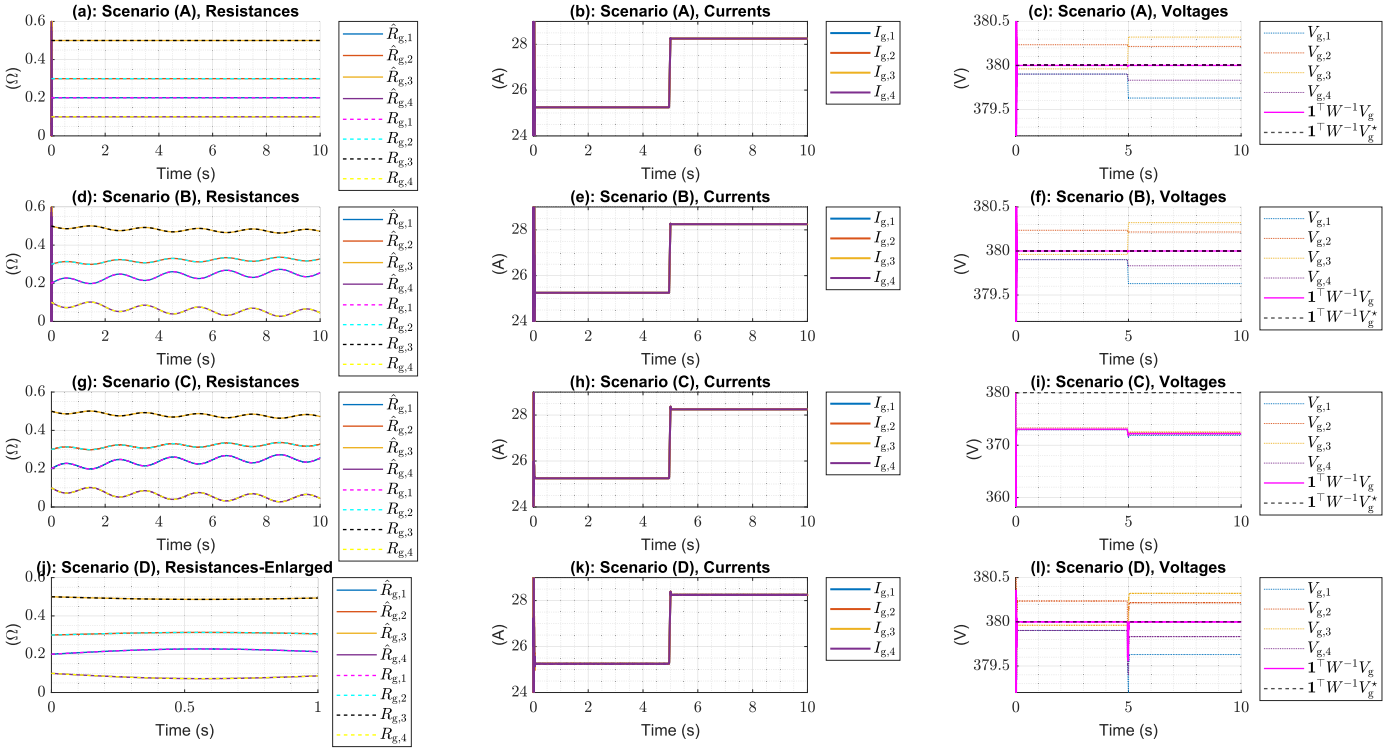

Fig. 3. Noise-free simulation. From top to the bottom: Scenario (A), Scenario (B), Scenario (C), and Scenario (D). Time histories of: **(Left:)** the components of the matrix R_g and the associated estimates $\hat{R}_g$. **(Centre:)** The currents I_g. **(Right:)** The voltages V_g, along with their weighted mean value $\mathbf{1}^\top W^{-1} V$ and the reference $\mathbf{1}^\top W^{-1} V_g^\star$.

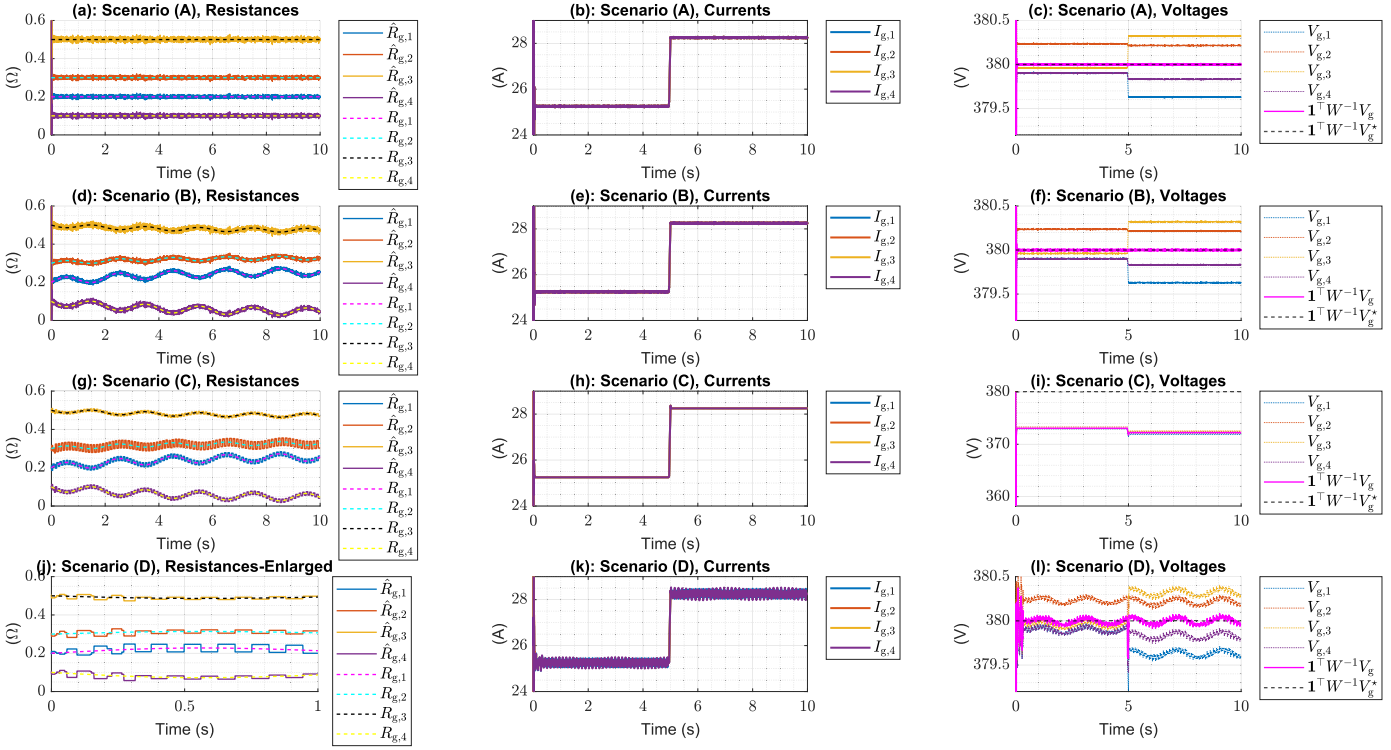

Fig. 4. Simulation with noise. From top to the bottom: Scenario (A), Scenario (B), Scenario (C), and Scenario (D). Time histories of: **(Left:)** the components of the matrix R_g and the associated estimates $\hat{R}_g$. **(Centre:)** The currents I_g. **(Right:)** The voltages V_g, along with their weighted mean value $\mathbf{1}^\top W^{-1} V$ and the reference $\mathbf{1}^\top W^{-1} V_g^\star$.

If we choose as base unit for the current 50 (A) and 500 (V) for the voltage, the associated injected measurement noises have a variance $w^2 = 0.01$ (p.u.).

During Scenario (A), the use of the control approach (9a)–(9d) ensures that a correct estimation of the constant matrix R_g is achieved asymptotically (Fig. 3(a)). Objectives 1 and 2 are also asymptotically achieved (Fig. 3(c,d)). If we consider in Scenario (B) time-varying perturbations on R_g, the performances of the control scheme (9a)–(9d) are still acceptably accurate (Fig. 3(d,e,f)), and the two control Objectives 1 and 2 are still achieved. The proposed

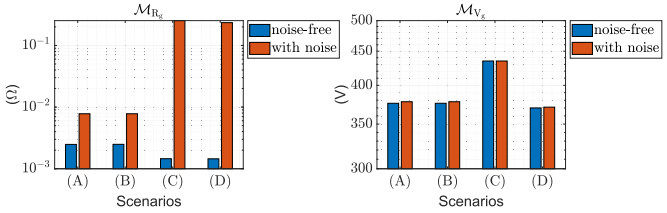

Fig. 5. The numerical values of the introduced RMSE performance metrics $\mathcal{M}_{R_g}$, $\mathcal{M}_{V_g}$ evaluated for the four scenarios, in absence and in presence of measurement noise.

STA-based scheme is capable of estimating R_g in finite time, as shown in Fig. 3(g). If we do not compensate online the fluctuations on R_g as per Scenario (C), we can still achieve current sharing Objective 1 (Fig. 3(h)), whilst the voltage balancing problem (Fig. 3(i)) is not achieved, as the weighted mean value of the voltage is far below the prescribed setpoint. To achieve both the current sharing (Objective 1), and voltage balancing (Objective 2), we use the proposed compensation scheme in Scenario (D), where all the objectives are achieved with the greatest accuracy. The analysis undertaken in Fig. 5 (noise-free scenario) suggests that the accuracy of the STA schemes is higher than the adaptive scheme in (10), by virtue of the enforced finite-time convergence to the origin of the error variables.

Fig. 4 summarises the results in presence of noise. Despite all the performance metrics record a slightly worsening of the accuracy in all the scenarios (see Fig. 5), the overall performance of the estimations of the resistances are still acceptable, and the control objectives are still achieved. It is interesting to observe that if we employ the scheme in (10) to estimate R_g, we observe that its accuracy degrades less than if we use (22f)–(22i).

5. Conclusion

In this paper, we have proposed two novel strategies to solve the problem of achieving current sharing and voltage balancing in DC microgrids in the scenario where DGU filter parasitic resistances are unknown and potentially time-varying. The first strategy refers to an adaptive control scheme that is able to solve the problem for the case of constant and unknown DGU filter parasitic resistances. We also considered the case of time-varying filter resistances, for which a second scheme inspired by SM STA was designed and was able to estimate in finite time the DGU resistances and tracking their evolution.

Declaration of Competing Interest

The authors declare that they have no known competing financial interests or personal relationships that could have appeared to influence the work reported in this paper.

Acknowledgements

Juan E. Machado gratefully acknowledges the financial support from the Dutch Research Council (NWO) under Grant ESI.2019.005 and the NWO, ERA-Net Smart Energy Systems and European Union's Horizon 2020 research and innovation programme under Grant 775970.

Gianmario Rinaldi and Prathyush P. Menon gratefully acknowledge the partial funding support from the Innovate UK Project *CMDC 2 ZERO - Zero Emission Research and Offshore Service Vessel* (Project number 122045).

Prathyush P. Menon gratefully acknowledges the partial funding support from the Innovate UK Project *Connected Secure In Cable Control and Protection Device for Electric Vehicle charging supporting mode 2 and 3 use* with EVParts UK Ltd. (Project number 80492).

References

[1] S. Ali, Z. Zheng, M. Aillerie, J.-P. Sawicki, M.-C. Pera, D. Hissel, A review of DC microgrid energy management systems dedicated to residential applications, Energies 14 (14) (2021) 4308.
[2] A. Astolfi, R. Ortega, Dynamic extension is unnecessary for stabilization via interconnection and damping assignment passivity-based control, Syst. Control Lett. 58 (2) (2009) 133–135.
[3] M. Cucuzzella, S. Trip, C. De Persis, X. Cheng, A. Ferrara, A. van der Schaft, A robust consensus algorithm for current sharing and voltage regulation in DC microgrids, IEEE Trans. Control Syst. Technol. 27 (4) (2019) 1583–1595.
[4] A. Ferrara, G.P. Incremona, M. Cucuzzella, Advanced and Optimization Based Sliding Mode Control: Theory and Applications, SIAM, 2019.
[5] F. Galvanin, M. Barolo, F. Bezzo, Online model-based redesign of experiments for parameter estimation in dynamic systems, Ind. Eng. Chem. Res. 48 (9) (2009) 4415–4427.
[6] J.M. Guerrero, R. Kandari, Microgrids: Modeling, Control, and Applications, Academic Press, 2021.
[7] Y. Kawano, M. Cucuzzella, S. Feng, J.M.A. Scherpen, Krasovskii and shifted passivity based output consensus Automatica, (2023) arXiv:2207.01430.
[8] H. Khalil, Nonlinear Control, Global Edition, Pearson, 2015.
[9] S.-B. Lee, T.G. Habetler, An online stator winding resistance estimation technique for temperature monitoring of line-connected induction machines, IEEE Trans. Ind. Appl. 39 (3) (2003) 685–694.
[10] J.E. Machado, M. Cucuzzella, N. Pronk, J.M.A. Scherpen, Adaptive control for flow and volume regulation in multi-producer district heating systems, IEEE Control Syst. Lett. 6 (2022) 794–799.
[11] L. Meng, Q. Shafiee, G.F. Trecate, H. Karimi, D. Fulwani, X. Lu, J.M. Guerrero, Review on control of DC microgrids and multiple microgrid clusters, IEEE J. Emerg. Sel. Top. Power Electron. 5 (3) (2017) 928–948.
[12] J.A. Moreno, Lyapunov approach for analysis and design of second order sliding mode algorithms, in: Sliding Modes After the First Decade of the 21st Century, Springer, 2011, pp. 113–149.
[13] S.P. Nageshrao, G.A.D. Lopes, D. Jeltsema, R. Babuška, Port-Hamiltonian systems in adaptive and learning control: a survey, IEEE Trans. Autom. Control 61 (5) (2016) 1223–1238, doi:10.1109/TAC.2015.2458491.
[14] P. Nahata, G. Ferrari-Trecate, On existence of equilibria, voltage balancing, and current sharing in consensus-based DC microgrids, in: Proc. European Control Conf. (ECC), St. Petersburg, Russia, 2020, pp. 1216–1223.
[15] V. Nasirian, A. Davoudi, F.L. Lewis, J.M. Guerrero, Distributed adaptive droop control for DC distribution systems, IEEE Trans. Energy Convers. 29 (4) (2014) 944–956.
[16] R. Ortega, E. Garcia-Canseco, Interconnection and damping assignment passivity-based control: a survey, Eur. J. Control 10 (5) (2004) 432–450.
[17] G. Rinaldi, J.E. Machado, M. Cucuzzella, P.P. Menon, A. Ferrara, J.M.A. Scherpen, Finite-time output parameter estimation for a class of nonlinear systems, IEEE Control Syst. Lett. 6 (2022) 3253–3258.
[18] G. Rinaldi, P.P. Menon, C. Edwards, A. Ferrara, Y. Shtessel, Adaptive dual-layer super-twisting sliding mode observers to reconstruct and mitigate disturbances and communication attacks in power networks, Automatica 129 (2021) 109656.
[19] Y. Shtessel, C. Edwards, L. Fridman, A. Levant, et al., Sliding Mode Control and Observation, vol. 10, Springer, 2014.
[20] S. Trip, M. Cucuzzella, X. Cheng, J.M.A. Scherpen, Distributed averaging control for voltage regulation and current sharing in DC microgrids, IEEE Control Syst. Lett. 3 (1) (2019) 174–179.
[21] M. Tucci, L. Meng, J.M. Guerrero, G. Ferrari-Trecate, Stable current sharing and voltage balancing in DC microgrids: a consensus-based secondary control layer, Automatica 95 (2018) 1–13.
[22] V. Utkin, Sliding mode control of DC/DC converters, J. Frankl. Inst. 350 (8) (2013) 2146–2165.